Contribution from the Central Research & Development Department,
Experimental Station, E. I. du Pont de Nemours & Company, Inc., Wilmington, Delaware 19898

Steric and Electronic Control of Iron Porphyrin Catalyzed Hydrocarbon Oxidations

Mario J. Nappa* and Chadwick A. Tolman

Received July 17, 1985

The yields and product distributions in the oxidation of hydrocarbons (cyclohexane, *n*-pentane, *n*-octane, methylcyclohexane, *tert*-butylcyclohexane, and ethylbenzene), using substituted iron tetraphenylporphyrins and iodosobenzene, are shown to be markedly affected by the nature and location of phenyl ring substituents. These substrates were used to measure the activity, regioselectivity, substrate selectivity, and stereoselectivity of our substituted iron porphyrin catalysts. Higher yields are observed with iron porphyrins having bulky substituents near the iron center. Kinetics measurements and concentration studies show that these substituents improve lifetimes by hindering the catalyst's bimolecular self-destruction. Higher yields are also observed with electron-withdrawing substituents. A new iron "fluoro-pocket" porphyrin shows high activity due to this electronic effect. Substrate and regioselectivity are also influenced by steric *and* electronic effects of the iron porphyrin's phenyl ring substituents. Bulky porphyrins also affect the stereoselectivity at the 2-, 3-, and 4-positions in *tert*-butylcyclohexane oxidation. A mechanism supported by kinetic modeling studies is proposed for the oxidation reactions.

Introduction

Cytochromes P-450 are a class of enzymes that catalyze the monooxygenation of a variety of organic substrates with the use of dioxygen and NADPH or single oxygen donors such as iodosoarenes.[1] The use of synthetic iron porphyrins as models for the enzyme in aliphatic hydroxylations is now firmly established; however, these models usually give low yields and poor selectivity. For example, Groves first reported that iron tetraphenylporphyrin chloride, Fe(TPP)Cl, catalyzes oxygen atom transfer from iodosobenzene to cyclohexane to give cyclohexanol, but only in 8% yield (based on iodosobenzene).[2] Mansuy was able to increase the yield to 19% by changing the solvent from methylene chloride to benzene and by using a higher concentration of cyclohexane.[3] It was also reported that in *n*-heptane oxidation, the reactivity can be directed toward the ends of the heptane molecule using iron complexes of "basket-handle" porphyrins.[3] Groves reported a 20% yield of cyclohexanol by using iron tetrakis(2-methylphenyl)porphyrin chloride and suggested that a steric effect from the 2-methyl substituents was responsible for this higher yield.[4] In later work, he reported modest effects on stereoselectivity in *cis*-decalin oxidation by using this catalyst.[5] Chang, using iron tetrakis(pentafluorophenyl)porphyrin chloride, attributed a high cyclohexanol yield of 71% to both steric and electronic effects of the fluorine substituents.[6] This iron porphyrin also catalyzes the oxidation of substituted aromatic substrates and exhibits a marked NIH shift reminiscent of those occurring in enzymatic systems. Traylor et al. have reported that iron tetrakis(2,6-dichlorophenyl)porphyrin chloride gives a high cyclohexanol yield of 73% with pentafluoroiodosobenzene as the oxidant and have shown that the chlorine substituents increase catalyst lifetimes, leading to high yields.[7]

Primary oxidants other than iodosobenzene have been reported to oxidize saturated hydrocarbons in the presence of iron porphyrins. Alkylhydroperoxides are effective,[8] but their reactions have been shown to proceed primarily via radicals.[3] Cyclohexane was oxidized by using hemin/ascorbic acid/dioxygen to give ~4% of cyclohexanol based on the amount of dioxygen consumed.[9] A similar system, hemin/thiosalicylic acid/dioxygen, gave ~2% of cyclohexanol based on the thiosalicylic acid present at the beginning of the reaction. The yield of cyclohexanol was insensitive to radical inhibitors, suggesting a mechanism for this system similar to that for iodosobenzene.[10]

Since understanding the factors that influence the yields of iron porphyrin catalyzed oxidations should lead to the development of more active and selective hydrocarbon oxidation catalysts, we carried out a systematic and detailed study, using tetraphenylporphyrin derivatives, of the relationships between iron porphyrin structure and activity and shape selectivity in the oxidations of cyclohexane, *n*-pentane, *n*-octane, methylcyclohexane, *tert*-butylcyclohexane, and ethylbenzene.

Results and Discussion

Cyclohexane Oxidation. Under mild conditions iron porphyrins catalyze oxygen transfer from iodosobenzene to saturated hydrocarbons, resulting in oxygen atom insertion into C–H bonds. The reaction between cyclohexane, iodosobenzene, and iron tetraphenylporphyrin in a molar ratio of 1100/20/1 at 25 °C results in the formation of cyclohexanol in 10% yield based on iodosobenzene. Under our conditions of high initial cyclohexane concentration, which results in low hydrocarbon conversion, we observe only trace amounts of cyclohexanone. The yield of cyclohexanol is critically dependent on the absolute and relative concentrations of the reactants and is also sensitive to both reaction conditions and phenyl ring substituents of the iron tetraphenylporphyrin catalysts.

The reaction between cyclohexane and iodosobenzene catalyzed by iron tetraphenylporphyrin derivatives is dependent on the initial concentration of cyclohexane, as shown in Figure 1. For accuracy, $Fe(T_{2\text{-}F}PP)Br$,[11] which gives higher yields of cyclohexanol, was used. The reaction is carried out in methylene chloride, and even

* To whom correspondence should be addressed at the Chemicals and Pigments Department, Jackson Laboratory, E. I. du Pont de Nemours & Co., Deepwater, NJ 08023.

(1) Coon, M. J.; White, R. E. "Metal Ion Activation of Dioxygen"; Spiro, T. G., Ed., Wiley: New York, 1980, Chapter 2. (b) Sligar, S. G.; Gunsales, J. C. *Adv. Enzymol. Relat. Areas Mol. Biol.* **1978**, *47*, 1. (c) Groves, J. T. *Adv. Inorg. Biochem.* **1979**, *1*, Chapter 4. (d) Chang, C. K.; Dolphin, D. *Bioorg. Chem.* **1978**, *4*, 37.
(2) Groves, J. T.; Nemo, T. E.; Meyers, R. S. *J. Am. Chem. Soc.* **1979**, *101*, 1032.
(3) Mansuy, D.; Bartoli, J. F.; Momenteau, M. *Tetrahedron Lett.* **1982**, *23*, 2781.
(4) Groves, J. T.; Kruper, W. J.; Nemo, T. E.; Meyers, R. S. *J. Mol. Catal.* **1980**, *7*, 169.
(5) Groves, J. T.; Nemo, T. E. *J. Am. Chem. Soc.* **1983**, 105, 6243.
(6) Chang, C. K.; Ebina, F. *J. Chem. Soc., Chem. Commun.* **1981**, 778.
(7) Traylor, P. S.; Dolphin, D.; Traylor, T. G. *J. Chem. Soc., Chem. Commun.* **1984**, 279.
(8) Mansuy, D.; Bartoli, J. F.; Chottard, J. C.; Lange, M. *Angew. Chem., Int. Ed. Engl.* **1980**, *19*, 909.
(9) Xianyuan, W.; Mengqin, Z.; Huahua, H.; Liangwen, G.; Quanjie, L.; Tinghui, X.; Guoyang, Z.; Guangnian, L. *Cuihua Xuebao* **1981**, *2*, 323.
(10) Belova, V. S.; Nikonova, L. A.; Raikman, L. M.; Borukayeva, M. R. *Dokl. Akad. Nauk SSSR* **1982**, *204*, 897.
(11) Abbreviations used in this paper: TPP, *meso*-tetraphenylporphyrin dianion; $T_{4\text{-}Me}PP$, *meso*-tetrakis(4-methylphenyl)porphyrin dianion; $T_{3\text{-}Me}PP$, *meso*-tetrakis(3-methylphenyl)porphyrin dianion; $T_{2\text{-}Me}PP$, *meso*-tetrakis(2-methylphenyl)porphyrin dianion; $T_{3,4,5\text{-}MeO}PP$, *meso*-tetrakis(3,4,5-trimethoxyphenyl)porphyrin dianion; $T_{2,4,6\text{-}MeO}PP$, *meso*-tetrakis(2,4,6-trimethoxyphenyl)porphyrin dianion; $T_{2\text{-}F}PP$, *meso*-tetrakis(2-fluorophenyl)porphyrin dianion; TF_5PP, *meso*-tetrakis(2,3,4,5,6-pentafluorophenyl)porphyrin dianion; FPP-3, *meso*-$\alpha,\alpha,\alpha,\alpha$-tetrakis(heptafluorobutyramidophenyl)porphyrin dianion; FPP-7, *meso*-$\alpha,\alpha,\alpha,\alpha$-tetrakis(perfluorooctanamidophenyl)porphyrin dianion; HPP-7, protio analogue of FPP-7; Pc, phthalocyanine dianion; FPc, perfluorophthalocyanine dianion; $H_2T_{AM}PP$, *meso*-tetrakis(2-aminophenyl)porphyrin.

0020-1669/85/1324-4711$01.50/0

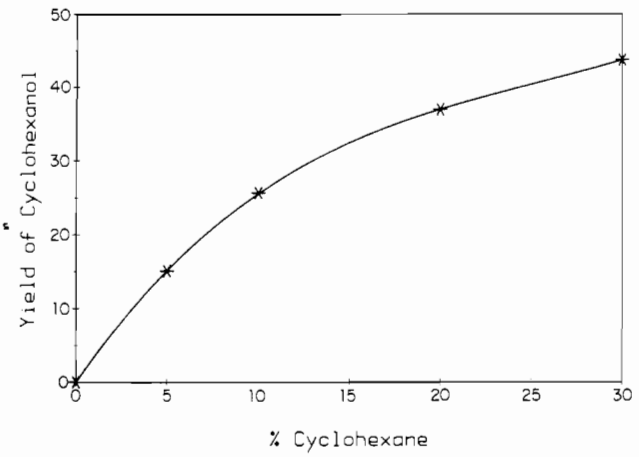

Figure 1. Yield of cyclohexanol (based on iodosobenzene used) vs. % cyclohexane in methylene chloride using Fe($T_{2\text{-}F}$PP)Br at 25 °C.

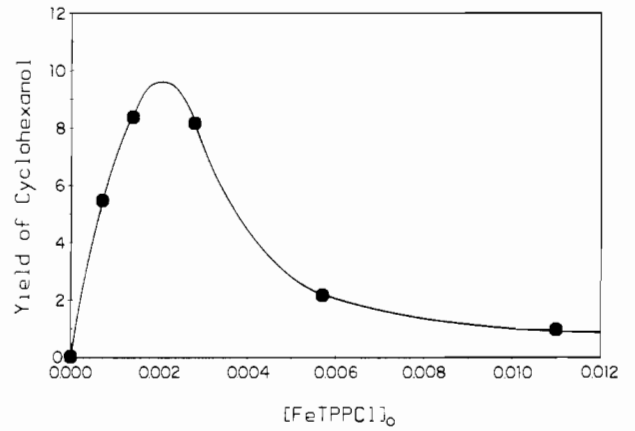

Figure 2. Catalyst concentration study: yield of cyclohexanol with 30% cyclohexane in CH_2Cl_2 at 25 °C vs. the initial concentration of Fe(TPP)Cl. Under standard conditions, the catalyst concentration was 0.0025 M.

at 30% cyclohexane (2.78 M), the yield has not reached a maximum. This can be explained by a mechanism involving a competitive oxidation of iodoso- to iodoxybenzene with the reactions

$$\text{PhIO} + \text{Fe} \xrightarrow{k_1} \text{PhI} + \text{OFe} \quad (1)$$

$$\text{OFe} + \text{CyH} \xrightarrow{k_2} \text{Fe} + \text{CyOH} \quad (2)$$

$$\text{OFe} + \text{PhIO} \xrightarrow{k_3} \text{Fe} + \text{PhIO}_2 \quad (3)$$

$$\text{OFe} + \text{Fe} \xrightarrow{k_4} \text{Fe} + \text{D} \quad (4)$$

The initial step is oxygen transfer from iodosobenzene to the iron(III)porphyrin to generate a high oxidation state ferryl intermediate. Groves et al. have spectroscopic evidence that this OFe complex is an (oxo)iron(IV) porphyrin π-cation radical.[5] The next three steps involve competitive reactions of this intermediate with cyclohexane to give the desired reaction, with iodosobenzene to give iodoxybenzene or with catalyst to give destroyed catalyst D.[12]

We know that reaction 3 competes with reaction 2 because in a reaction using Fe($T_{2\text{-}F}$PP)Br, iodoxybenzene was isolated at the end of the reaction, characterized by IR, and weighed. Almost all (~90%) of the iodosobenzene was accounted for. Our preliminary kinetic modeling studies indicate that k_3/k_2 is approximately equal to 10^4, making a direct study of reaction 3 in the absence of substrate and with standard techniques impossible. Such a study would also be complicated by mass-transfer effects (dissolution of iodosobenzene). We known that reaction 4 takes place because we observe iron porphyrin decomposition when the vis/UV spectra are monitored during oxidation reactions. Evidence for bimolecular catalyst destruction comes from catalyst concentration and kinetic studies.

(12) In most cases the catalysts decolorize within 15–20 min, indicating destruction of the porphyrins. We have not characterized the products of catalyst oxidation.

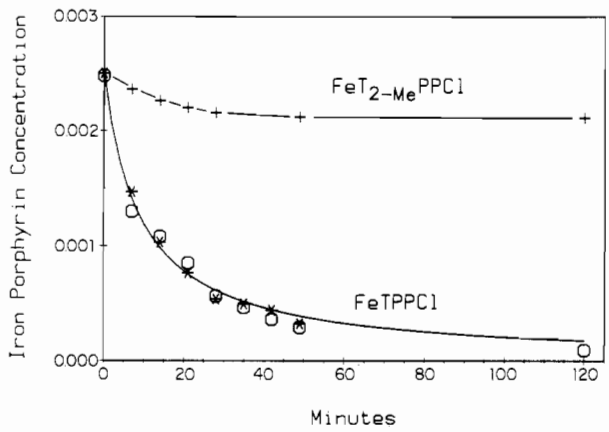

Figure 3. Iron porphyrin decomposition: iron porphyrin concentration measured by vis/UV spectroscopy vs. time at 2 °C for Fe(TPP)Cl (○ and ★) and Fe($T_{2\text{-Me}}$PP)Cl (+).

Table I. Cyclohexane Oxidation: Cyclohexanol Yields for Different Iron Porphyrin Derivatives

iron porphyrin	cyclohexanol yield[a]	iron porphyrin	cyclohexanol yield[a]
Fe($T_{4\text{-Me}}$PP)Cl	6.9 ± 0.4	Fe(FPP-3)Cl	39.4 ± 0.4
Fe($T_{3\text{-Me}}$PP)Cl	7.9 ± 0.1	Fe(FPP-3)Br	36.7 ± 0.2
Fe($T_{2\text{-Me}}$PP)Cl	31.7 ± 1.0	Fe(FPP-7)Br	36.7 ± 0.6
Fe($T_{3,4,5\text{-MeO}}$PP)Cl	23.1 ± 0.5	Fe(HPP-7)Br	21.7 ± 0.7
Fe($T_{2,4,6\text{-MeO}}$PP)Cl	13.0 ± 1.2	FePc	30.8 ± 0.7
Fe($T_{2\text{-F}}$PP)Cl	48.4 ± 0.2	FeFPc	11.0 ± 0.4
Fe(TF_5PP)Cl	66.6 ± 1.0	Fe(TPP)Cl	10.1 ± 0.1

[a] Based on iodosobenzene oxidant charged. 30% cyclohexane in CH_2Cl_2 was vigorously stirred at ambient temperature for 2 h.

The effect of varying the concentration of Fe(TPP)Cl on the yield of cyclohexanol in the oxidation of cyclohexane is shown in Figure 2. The yield, based on iodosobenzene, starts out low because at low initial catalyst concentrations the iodosobenzene is not completely consumed before the catalyst is destroyed; as the initial catalyst concentration is increased, the yield increases until a maximum is reached at about 2.5×10^{-3} M (normal reaction conditions). As the concentration of the catalyst is increased further, the yield drops because at these high catalyst concentrations the catalyst itself acts as a substrate that effectively competes with the cyclohexane for the active ferryl intermediate (reaction 4 of the proposed mechanism).

In spite of the low solubility of iodosobenzene in the reaction medium, we were able to carry out reproducible kinetic measurements at 2 °C by monitoring the loss of the iron porphyrin (by vis/UV). Figure 3 shows the results of two kinetic runs using Fe(TPP)Cl and one using Fe($T_{2\text{-Me}}$PP)Cl. The decomposition of Fe(TPP)Cl follows second-order kinetics with an apparent rate constant of 44 M^{-1} s^{-1}, supporting reaction 4 of the proposed mechanism. On the other hand, with Fe($T_{2\text{-Me}}$PP)Cl there is little decomposition (15%), and its initial rate is much slower than with Fe(TPP)Cl, indicating that the *o*-methyl groups of Fe($T_{2\text{-Me}}$PP)Cl hinder its bimolecular self-destruction. We monitored the formation of cyclohexanol, and the end of this reaction coincides with the end of iron porphyrin (Fe($T_{2\text{-Me}}$PP)Cl) destruction; this is most likely due to the depletion of iodosobenzene. We observe less iron porphyrin degradation with this catalyst at 2 °C than at room temperature, and also get a higher yield (50% at 2 °C vs. 32% at 25 °C).

In Table I, we show that the cyclohexanol yield (based on iodosobenzene) for reactions carried out under standard conditions

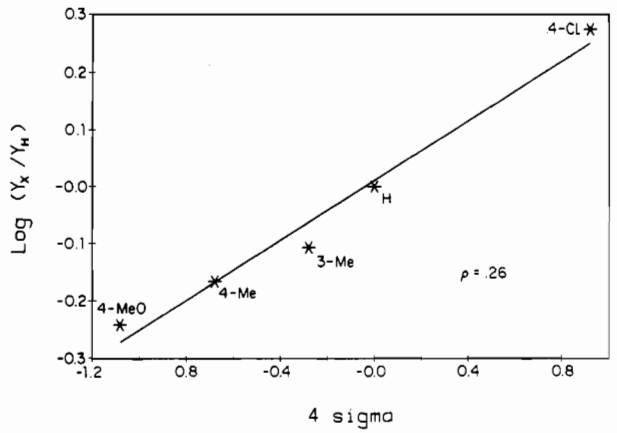

Figure 4. Hammett plot for the log (Y_X/Y_H) [Y_X = yield of cyclohexanol (ROH) for Fe($T_{3\text{-}X}$PP)Cl or Fe($T_{4\text{-}X}$PP)Cl. Y_H = yield of ROH for Fe(TPP)Cl] vs. 4σ for the phenyl ring substituent.

depends on the nature and location of substituents in a series of iron tetraphenylporphyrin derivatives of the type

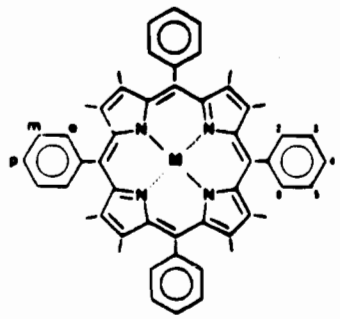

All our iron porphyrin catalysts have the same substituent(s) on each phenyl ring, and unless specified otherwise, the tetra-2-substituted porphyrins are atropisomeric mixtures. A plot of the log of yield with substituted iron porphyrin relative to that with Fe(TPP)Cl [log (Y_X/Y_H)] vs. 4σ (there are four substituents per porphyrin) clearly shows that electron-withdrawing substituents increase the cyclohexanol yield (Figure 4), with a ρ value of 0.26 ± 0.02. (A ρ value of 0.35 ± 0.06 was obtained for the production of *sec*-phenethanol in the oxidation of ethylbenzene.) The nature of this effect may be 2-fold. First, electron-withdrawing groups may activate the ferryl intermediate and increase its reactivity toward hydrocarbon more than toward iodosobenzene (increase k_2/k_3). Second, the substituents, by removing electron density from the ring, make the porphyrin less susceptible to electrophilic attack (decrease k_4 and give longer catalyst lifetimes). Evidence for the latter comes from measuring the extent of iron porphyrin decomposition by vis/UV at the end of the reactions: Fe($T_{2\text{-Cl}}$PP)Cl, 74%; Fe(TPP)Cl, 88%; Fe($T_{4\text{-Me}}$PP)Cl, 86%;: Fe($T_{4\text{-MeO}}$PP)Cl, 93%. The extent of decomposition was also measured for Fe($T_{2\text{-Me}}$PP)Cl (71%). In this series, this catalyst gave the highest yield of cyclohexanol and also had the longest lifetime. Apparently, this is due to the methyl groups retarding bimolecular self-destruction (decreasing k_4).

We can distinguish between steric and electronic effects on cyclohexanol yield by the plot shown in Figure 5. Here the yield term [log (Y_X/Y_H)] is plotted against the electrochemical potential for ring oxidation[13] of the Fe(III) chloride complexes. The plot is linear for the Hammett series and a new "fluoro-pocket" porphyrin complex, iron *meso*-$\alpha,\alpha,\alpha,\alpha$-tetrakis(heptafluorobutyramidophenyl)porphyrin chloride, abbreviated FPP-3, and clearly shows that it is the electron-withdrawing nature of the perfluoro amide groups, and not a steric effect, that is responsible for its enhanced activity. Moreover, increasing the fluorocarbon chain

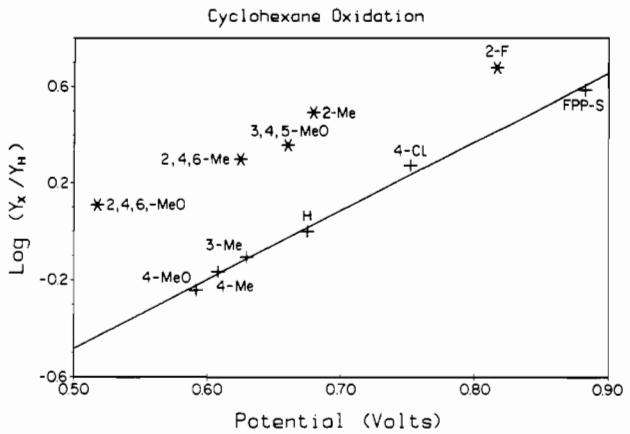

Figure 5. Steric and electronic effects on the yield: log (Y_X/Y_H) vs. the porphyrin ring oxidation potentials, measured in CH_2Cl_2 (0.2 M tetrabutylammonium tetrafluoroborate) vs. SCE and referenced to internal ferrocene.

Table II. Effect of Axial Ligand on Cyclohexanol Yield for Fe(TPP)X Catalysts

X^-	ClO_4^-	MeO^-	Br^-	Cl^-	F^-
cyclohexanol yield[a]	<1	8	8	10	12
$E_{1/2}(Fe^{III}/Fe^{II})$, V	0.22		−0.21	−0.29	−0.50

[a] Based on iodosobenzene, ± 1%.

length has no effect on cyclohexanol yield (Table I). The vertical distances of points above the line give a measure of steric effects. It appears as though the steric effects are approximately the same for any substituent, which is not totally surprising since these steric groups are preventing the bimolecular destruction of the catalyst (face to face approach), and even a small substituent such as fluoride is effective. This evidence argues against any large contribution to the yield loss due to intramolecular decomposition of the catalyst where the measured steric effect should be more a function of the size of the substituent.

Varying the axial ligand in an Fe(TPP)X series causes the yields of cyclohexanol in the oxidation of cyclohexane to decrease in the series $F^- > Br^- > CH_3O^- > Cl^- > ClO_4^-$ (Table II). The complex with the most negative Fe(III)/Fe(II) potential gives the highest yield. Kadish explained the trend in redox potentials by proposing that for this series the iron–fluoride bond is the strongest; therefore, fluoride stabilizes high oxidation states, and the complex has the most negative Fe(III)/Fe(II) potential; the iron–perchlorate complex has the weakest bond and the most positive potential.[14] We can explain the higher activity for the fluoride complex because in its resting state this catalyst is more resistant to attack. Because of the weak bond, perchlorate offers little protection from bimolecular self-destruction of the catalyst, and this is verified by a visual inspection of a reaction solution using Fe(TPP)ClO_4. Kadish also reports that for these complexes the Fe(III)P/Fe(III)$P^{+\cdot}$ potential is unchanged by changing X, so the effect seen here is different from the porphyrin substituent electronic effect.

Some cyclohexyl chloride is observed in the oxidation when iron porphyrin bromide catalysts are used in methylene chloride, indicating that solvent participation also occurs, though only to a small extent; trace amounts of cyclohexyl bromide are also formed. We also observe trace amounts of cyclohexene oxide, resulting from the epoxidation of cyclohexene. If dioxygen is purged through the solution at the start of the reaction, cyclohexyl halides to not form but cyclohexene does; apparently the dioxygen intercepts the cyclohexyl radical before it can react with solvent or catalyst. The presence of cyclohexyl radicals supports an initial hydrogen atom abstraction pathway for reaction 2.[5] The cyclohexene cannot be generated from the disproportionation of cyclohexyl radicals (which would be rapidly captured by O_2), but must form from an intracage process resulting in the oxidative

(13) The site of oxidation may be the porphyrin ring and the iron in the +3 oxidation state: Groves, J. T.; Quinn, R.; McMurray, T. J.; Lang, G.; Boso, B. *J. Chem. Soc., Chem. Commun.* **1984**, 1455.

(14) Phillippi, M. A.; Goff, H. M. *J. Am. Chem. Soc.* **1982**, *104*, 6026.

dehydrogenation of cyclohexane. The ratio of cyclohexene oxide/cyclohexanol is higher for catalysts with electron-withdrawing fluorine substituents. For example, Fe($T_{2\text{-}F}$PP)Cl and Fe(TF_5PP)Cl give a cyclohexene oxide/cyclohexanol ratio of ~0.03. These groups promote electron-transfer by making FeP(OH)X a better oxidizing agent. Much less cyclohexene oxide is seen with other catalysts.

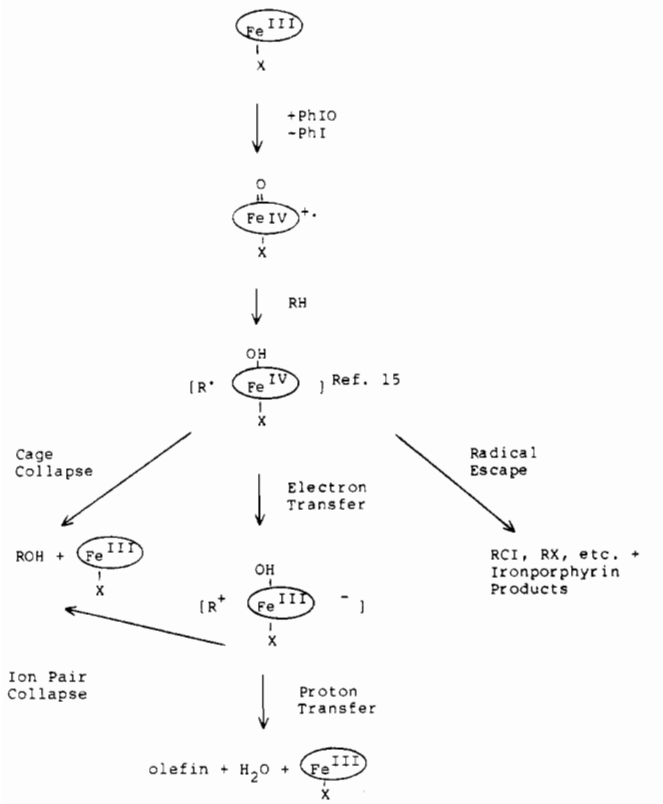

*The site of oxidation may be the porphyrin ring and the iron in the +3 oxidation state.[13]

We looked at the effect of pyridine on the yield in the oxidation of cyclohexane because of the possibility of using axial bases to protect the open face of the iron fluoropocket porphyrin catalysts. Addition of pyridine (0.5% of the total volume) reduces the yield of cyclohexanol with Fe(TPP)Cl from ~10% to ~7%. This is either because pyridine can convert the complex to an inactive form [Fe(TPP)$(py)_2$Cl], or because it can compete with hydrocarbon and be oxidized to pyridine *N*-oxide. We favor the former because 0.5% pyridine is enough to convert all of the Fe(TPP)Cl to the low-spin bis(pyridine) adduct[16] and because pyridines increase the efficacy of manganese porphyrin catalysts in the oxidation of saturated hydrocarbons.[17] We have found pyridine *N*-oxide to be unreactive as an oxygen atom transfer reagent under these conditions. We also observed no effects of a pyridine on the regioselectivity of Fe(FPP-3)Cl in pentane oxidation even when we preformed the Fe(FPP-3)(*t*-Bupy)Cl complex at −78 °C and carried out the oxidation at low temperatures.[18]

In order to evaluate the effect of fluorine substitution, we tried iron perfluorophthalocyanine as an oxidation catalyst. As shown in Table I, we observed a decrease in yield from that with the protio analogue under our standard reaction conditions, but this is most likely due to the low solubility of FeFPc in our solvent system.

Pentane and Octane Oxidations. Pentane was oxidized by using substituted iron tetraphenylporphyrins under standard conditions to give a mixture of 1-, 2-, and 3-pentanols and trace amounts of 2- and 3-pentanones (Table III). Worth noting is the reproducibility of the 2-/3-pentanol ratio, which can be used as a measure of the shape selectivity of a particular iron tetraphenylprophyrin derivative. The total product yields follow the same relative ordering of catalyst found for cyclohexane and ethylbenzene. Some typical yields for total pentanols are ~30% for Fe($T_{2\text{-}F}$PP)Br, 19% for Fe(FPP-3)Br, and 3% for Fe($T_{4\text{-}MeO}$PP)Cl.

Table III. 2-/3-Pentanol Ratios for Substituted Iron Tetraphenylporphyrins

iron porphyrin	2-/3-pentanol ratio (±0.02)	iron porphyrin	2-/3-pentanol ratio (±0.02)
Fe($T_{4\text{-}Me}$PP)Cl	1.61	Fe(FPP-7)Cl	1.84
Fe($T_{3,4,5\text{-}MeO}$PP)Cl	1.61	Fe($T_{2\text{-}F}$PP)Cl	2.08
Fe($T_{4\text{-}MeO}$PP)Cl	1.62	Fe(TF_5PP)Cl[a]	2.19
Fe(TPP)Cl	1.72	Fe($T_{2\text{-}Me}$PP)Cl	2.47
Fe($T_{4\text{-}Cl}$PP)Cl	1.73	Fe($T_{2,4,6\text{-}MeO}$PP)Cl	2.53
Fe($T_{3\text{-}Me}$PP)Cl	1.82	Fe($T_{2,4,6\text{-}Me}$PP)Cl	3.82
Fe(FPP-3)Cl	1.84		

[a] Gives a 1-/3-pentanol ratio of 0.07.

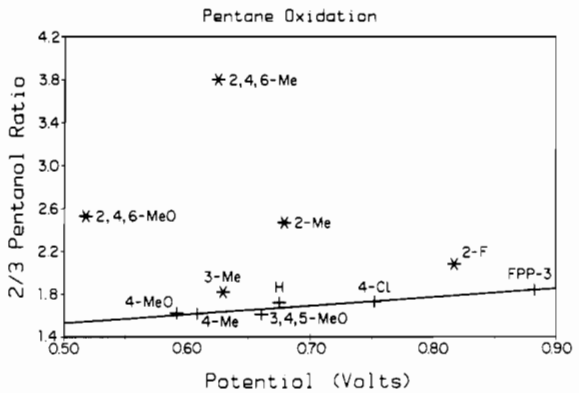

Figure 6. Steric and electronic effects on regioselectivity: 2-/3-pentanol ratio vs. the porphyrin ring oxidation potentials, measured in CH_2Cl_2 (0.2 M tetrabutylammonium tetrafluoroborate) vs. SCE and reference to internal ferrocene.

The 2-/3-pentanol ratio varied from 1.61 to 3.82, depending on the nature and location of the substituents (Table III); a ratio of 2.0 (4/2) is expected for totally random attack on pentane. For the first five entries, a small electronic effect is evident since the ratio is lowest for the *p*-methyl substituent and highest for the chloro, the most electron-withdrawing substituent in the para-substituted series.[19a]

This electronic effect is nicely shown by plotting the 2-/3-pentanol ratio vs. the porphyrin$^{+\cdot}$ redox potential (Figure 6). Notice that FPP-3 and $T_{3,4,5\text{-}MeO}$PP are collinear with the para-substituted series, indicating that the relatively high ratio for FPP-3 is due solely to an electronic effect. Moreover, increasing the fluorocarbon chain length had no effect on the 2-/3-pentanol ratio. We also observed the same ratio for Fe(FPP-3)OFe(FPP-3) suggesting that the μ-oxo linkage is labile under reaction conditions.[19b] The low ratio for Fe($T_{3,4,5\text{-}MeO}$PP)Cl suggests that the 3,5-methoxy groups are bent back away from the iron center and do not appreciably interact with the approaching pentane molecule.[20] While the substituents are far enough away so as not to influence reactions occurring at the iron center, they do play a

(15) Bottomly, L. A.; Kadish, K. M. *Inorg. Chem.* **1981**, *20*, 1348.
(16) Walker, F. A.; Lo, M.-W.; Ree, M. T. *J. Am. Chem. Soc.* **1976**, *98*, 5552.
(17) Nappa, M. J., unpublished results.
(18) Doeff, M. M.; Sweigart, D. A. *Inorg. Chem.* **1982**, *21*, 3699. Tondreau, G. A.; Sweigart, D. A. *Inorg. Chem.* **1982**, *23*, 1060.
(19) (a) Steric effects on reactivity of 2° sites have been noted by Groves in ref 5. (b) A similar observation was made by Groves et al. **1983**, (Groves, J. T.; Meyers, R. S. *J. Am. Chem. Soc.* **1983**, *105*, 5791), except that their synthetic procedure and spectral data suggest they had a hydroxo complex and not a μ-oxo dimer. A contrasting observation was made by Chang et al. (Chang, C. K.; Kuo, M.-S. *J. Am. Chem. Soc.* **1979**, *101*, 3413), their data suggesting that the μ-oxo dimer remained intact during oxidation reactions.
(20) A similar observation was made by: Latos-Grazynski, L.; Cheng, R.-J.; La Mar, G. N.; Balch, A. L. *J. Am. Chem. Soc.* **1982**, *104*, 5992.

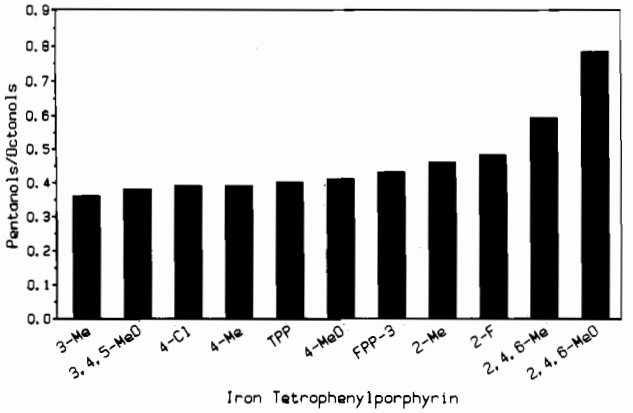

Figure 7. Competition experiment using cooxidation of pentane (1.08 M) and octane (1.08 M): total pentanols/total octanols ratios for different iron porphyrin catalysts.

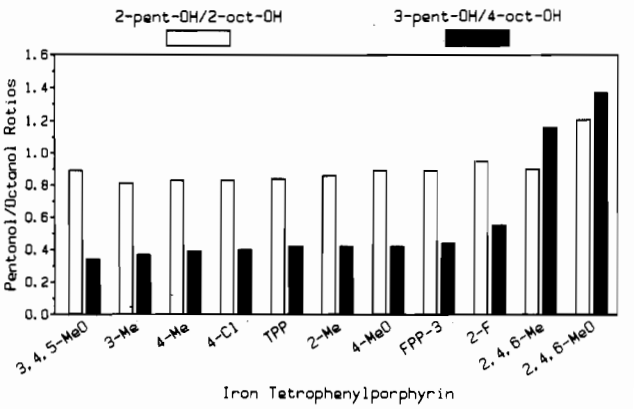

Figure 8. Competition experiment using cooxidation of pentane (1.08 M) and octane (1.08 M): 2-pentanol/2-octanol and 3-pentanol/4-octanol ratios for different iron porphyrin catalysts.

role in preventing the bimolecular destruction of iron porphyrin.

The reactive intermediate is believed to be an iron(IV) porphyrin π-cation radical.[21] The unpaired electron density residues on the oxygen in p-π–dπ antibonding orbitals approximately parallel to the porphyrin plane, giving the ferryl species oxy radical character. Electron-withdrawing groups on the porphyrin would be expected to make the oxy radical more reactive and less selective. The inductive release from two ethyl groups is expected to be slightly greater than from one methyl and one propyl,[22] favoring the 3-position over the 2-position for a relatively selective oxy radical. As the ferryl becomes more reactive the ratio should approach a value of 2.0 as it does with FPP-31 (1.84). We observed a more pronounced electronic effect of this nature in the oxidation of *tert*-butylcyclohexane (vide infra).

In addition to this electronic effect is the steric effect, the magnitude of which is indicated by the vertical distance between the starred points and the line in Figure 6. As expected, the following order is observed for the steric effect: 2,4,6-Me > 2,4,6-MeO > 2-Me > 2-F > 3-Me. 2,4,6-Me and 2,4,6-MeO give higher ratios because there are substituents above and below the prophyrin plane, unlike the other derivatives, which are atropisomeric mixtures. Fe(TF_5PP)Cl gave some 1-pentanol (1-/3-pentanol = 0.07), while with most of the catalysts little or no 1-pentanol was observed.

We also looked for substrate selectivity by carrying out cooxidations of pentane and octane present in equimolar amounts. Figure 7 shows the (total pentanol)/(total octanol) ratio for different iron porphyrin catalysts. With these catalysts there was essentially no terminal methyl group oxidation, so that a ratio of 0.5 (three CH_2's in pentane vs. six in octane) would be expected with no substrate selectivity. With the nonhindered porphyrin catalysts, there is an unexpected preference for octane over pentane. A similar observation has been made by Herron in cooxidations carried out with zeolite-encapsulated oxidation catalysts.[23] With substituents as the ortho positions there is more of a preference for pentane, the smaller of the two substrates. Porphyrins having substituents at both 2- and 6-positions show higher substrate selectivity, since now both faces are protected.

The effects are more pronounced when reactivities at the internal positions during competitive oxidations are compared, as shown in Figure 8. The 2-pentanol/2-octanol ratios are similar for all of the catalysts except Fe($T_{2,4,6\text{-MeO}}PP$)Cl. This indicates

Figure 9. Regioselectivity in methylcyclohexane oxidation: relative percents of the four alcohols (cis and trans are combined) for different iron porphyrin catalysts.

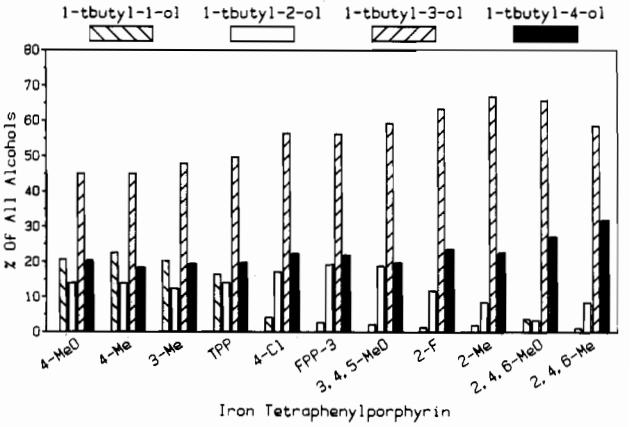

Figure 10. Regioselectivity in *tert*-butylcyclohexane oxidation: relative percents of the four alcohols (cis and trans are combined) for different iron porphyrin catalysts.

that both substrates can orient themselves to minimize repulsive interactions during reactions at the 2-positions.

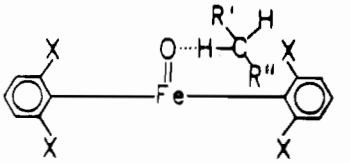

Varying R′ from an *n*-propyl group to an *n*-hexyl group (R″ = methyl) should have little effect on selectivity since R′ is directed away from the X substituents on the porphyrin's phenyl rings. However, when the 3-pentanol/4-octanol ratios are compared,

(21) Loew, G. H.; Kert, C. J.; Hjelmeland, L. M.; Kirchner, R. F. *J. Am. Chem. Soc.* **1977**, *99*, 3534. (b) Tatsumi, K.; Hoffmann, R. *Inorg. Chem.* **1981**, *20*, 3771. (c) Goddard, W. A., III, private communication.
(22) March, J. "Advanced Organic Chemistry"; McGraw-Hill: New York, 1968; p 19.
(23) Herron, N., unpublished results.
(24) Trotman-Dickenson, A. F. *Adv. Free-Radical Chem.* **1965**, *1*, 1.
(25) Bennett, J. E., Brown, D. M.; Mile, B.; *Trans. Faraday Soc.* **1970**, *66*, 386.
(26) Ullrich, V. *Angew. Chem., Int. Ed. Engl.* **1972**, *11*, 701.

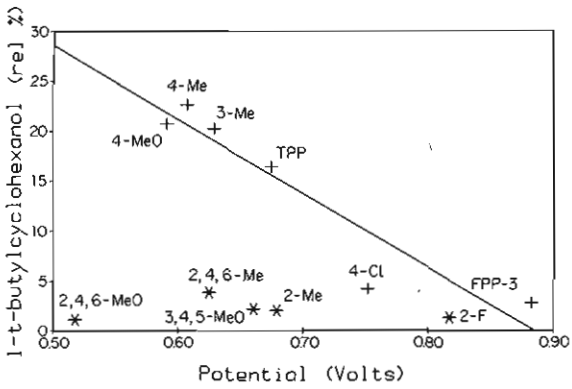

Figure 11. Steric and electronic effects on regioselectivity in *tert*-butylcyclohexane oxidation. The % *l-tert*-butylcyclohexanol is plotted vs. the porphyrin ring oxidation potential, measured in CH_2Cl_2 (0.2M tetrabutylammonium tetrafluoroborate) vs. *SLE* and referenced to internal ferrocene.

Table IV. Relative Reactivities for H Atom Abstraction from Hydrocarbons

attacking radical	temp, °C	1°	2°	3°
HO·[a]	17.5	1	4.7	9.8
t-BuO·[a]	40	1	10	44
RO_2·[b]	20	1	18	134
cytochrome P-450[c]	30	1	25	150

[a] From ref 24. [b] From ref 25; RO_2· = $CH_3CH_2CH_2(CH_3)HCO_2$·. [c] From ref 26.

there is a significant preference for the smaller substrate with the sterically crowded porphyrins.

Methyl- and *tert*-Butylcyclohexanes. Steric effects on site selection within the same molecule are nicely shown with methylcycylohexane (Figure 9). With increasing steric bulk on the porphyrin's phenyl rings, oxidations move toward the less sterically hindered 3- and 4-positions. (A 2/1 ratio would be expected on a statistical basis.) Fe($T_{2,4,6\text{-Me}}$PP)Cl is more selective than Fe($T_{2,4,6\text{-MeO}}$PP)Cl and Fe($T_{2\text{-Me}}$PP)Cl more than Fe($T_{2\text{-F}}$PP)Cl, the same ordering we observed for these catalysts in pentane oxidation.

A comparison of Figures 9 and 10 shows that increasing the size of the substituent on cyclohexane from methyl to *tert*-butyl shifts the oxidations more to the 3- and 4-positions, and now with the steric porphyrins and *tert*-butylcyclohexane little oxidation occurs at the 1- and 2-positions.

Steric and electronic effects in *tert*-butylcyclohexane oxidation are shown in Figure 11; there the % *l-tert*-butylcyclohexanol is plotted vs. the ring oxidation potential. Because of the bulky *tert*-butyl group, virtually any steric porphyrin substituent precludes reaction at the 1-position. However, we do observe an electronic effect with the meta- and para-monosubstituted porphyrins and the fluoro-pocket porphyrin. There is more reactivity at the 1-position with iron porphyrins having electron-donating substituents, because these substituents make the iron–oxo intermediate less reactive and more selective. With electron-withdrawing groups, the iron–oxo intermediate is more reactive and less selective for the more reactive tertiary hydrogen at the 1-position. This is consistent with the electronic effect we observed in pentane oxidation and with the relative reactivities/selectivities of oxygen-centered radical species in Table IV. As the reactivity of the oxygen-centered radical decreases, it becomes more selective for the 3° positions. Relative to the other oxygen-center radicals, cytochrome P-450 shows the greatest preference of the more reactive tertiary positions. Its substrate in Table IV was 2-methylbutane; however, with larger substrates steric interactions can dominate, and there is a preference for reactivity at the 1° terminal methyl groups of long linear alkanes.[27]

With *tert*-butylcyclohexane we observe stereoselectivity as shown in Figure 12. With increasingly bulky porphyrins, there

(27) Cardini, G.; Jurtshuk, P. *J. Biol. Chem.* **1970**, *245*, 2789.

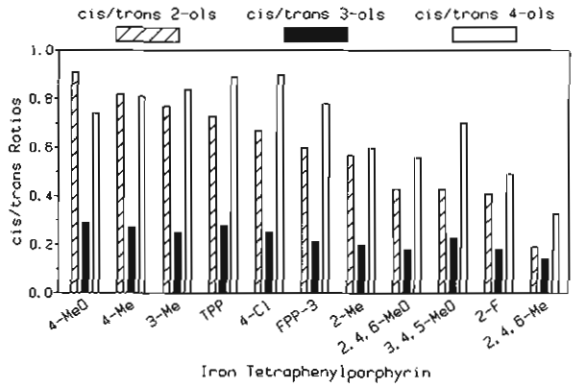

Figure 12. Stereoselectivity in *tert*-butylcyclohexane oxidation: cis/trans ratios for 2-, 3-, and 4-*tert*-butylcyclohexanols.

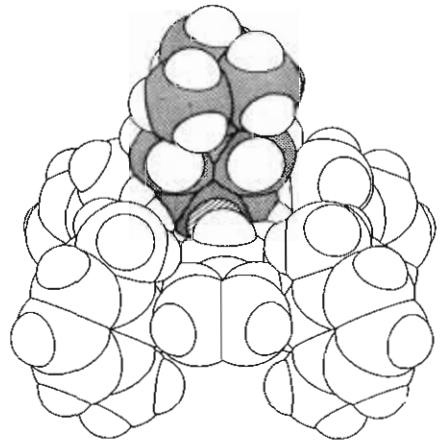

Figure 13. Computer-generated CPK model showing a linear C–H···O interaction for the 4-cis hydrogen atom (hatched) in *tert*-butylcyclohexane and the oxo ligand or iron.

is an increasing preference for the trans isomers, especially at the 2- and 4-positions. CPK space-filling models suggest that there is less steric hinderance by the methyl groups of Fe($T_{2,4,6\text{-Me}}$PP)Cl for an approach to the oxo ligand, parallel to the porphyrin plane, by the 4-cis hydrogen than by the 4-trans hydrogen. Figure 13 shows a computer-generated space-filling model with a linear C–H···O interaction for the 4-cis hydrogen. Considerably larger van der Waals interactions are evident for a similar approach of the 4-trans hydrogen. If this model for C–H approach is correct, then our observation of preferential trans hydroxylation at the 4-position is the result of stereoselectivity in the alcohol-forming step rather than in the C–H abstraction step. Formation of the 4-*tert*-butylcyclohexyl radical (or the 4-*tert*-butylcyclohexyl carbonium ion product of electron transfer) should result in complete loss of stereochemistry at the 4-position, but because of the steric effects imposed by the porphyrin ligand, there must be a preferential internal return of the hydroxyl (radical cage collapse or ion pair collapse) to form predominantly the 4-trans alcohol. All that is required for an 80/20 trans/cis mixture is a 1 kcal/mol difference in activation energies for the collapse reactions—not unreasonable values to expect from these steric effects.[28]

Iron Fluoro-Pocket Porphyrin Synthesis and Characterization. A new class of porphyrins, nicknamed the "fluoro-pocket" porphyrins, was made by modifying Collman's picket-fence porphyrin synthesis. *meso*-$\alpha,\alpha,\alpha,\alpha$-Tetrakis(heptafluoro-butyramidophenylporphyrin), FPP-3,[29] was made by reacting heptafluorobutyrylchloride with *meso*-$\alpha,\alpha,\alpha,\alpha$-tetrakis(*o*-aminophenyl)-porphyrin). Collman's method for inserting iron into picket-fence porphyrins (ferrous bromide in refluxing THF)[30] was not successful

(28) Lehr, G. F. Ph.D. Thesis, Brown University, 1981; p 134.
(29) The "3" signifies a linear three-carbon chain.
(30) Collman, J. P.; Gagne, R. R.; Reed, C. A.; Halbert, T. R.; Lang, G.; Robinson, W. T. *J. Am. Chem. Soc.* **1975**, *97*, 1427.

Table V. NMR of Ortho-Substituted Porphyrins

	Statistical Distribution	Type	Adjacent Interactions	Distant Interaction
	1	#1	↑↑	↑
	4	#2	↑↓	↑
		#3	↑↑	↓
		#4	↓↓	↓
	1	#5	↓↓	↑
	2	#6	↑↓	↓

for the fluoro-pocket porphyrins. Iron was inserted by using ferrous acetate in refluxing acetic acid, but TLC showed that atropisomerization had occurred. At 80 °C commercial ferrous bromide in benzene/THF (1/1) did not insert into H_2FPP-3. However, $FeBr_2$·2THF, essentially a pure form of ferrous bromide, inserted within 2 h. The iron fluoro-pocket porphyrin was then chromatographed to remove unreacted H_2FPP-3 and treated with HBr or HCl to make the corresponding halide complex. This method was used to make Fe(FPP-3)X, Fe(FPP-7)Br, Fe(HP-P-7)Br as well as Fe($T_{2\text{-}F}$PP)X where X is Br or Cl.

Fluorine NMR was used in characterizing the fluoro-pocket porphyrins. We were able to identify and quantify all of the atropisomers in a mixture (vide infra), to identify components in a mixture of iron fluoro-pocket porphyrin compounds in reactions of Fe(FPP-3)X with hydroxide, and to see chemical shift differences caused by the anions Cl^- or Br^- in our iron(III) complexes. (^{19}F chemical shifts are reported in the Experimental Section.) Fortunately, in fluorocarbons 1,3-couplings are greater than 1,2-couplings and the internal CF_2 resonance of α^4-FPP-3 appears as a singlet. However, in an atropisomeric mixture there are six magnetically inequivalent internal CF_2 groups, as shown in Figure 14. These internal CF_2 groups can be categorized by the orientation of adjacent and distant internal CF_2 groups (Table V), and as predicted there are three groups of two resonances. By NMR integration we found the relative amounts of atropisomers to be as follows: α^4, 0.1; $\alpha^3\beta$, 4.0; $\alpha\beta\alpha\beta$, 1.0; $\alpha^2\beta^2$, 1.7. The FPP-3 mixture was made from a mixture of $H_2T_{AM}PP$ atropisomers, which may have been depleted in the α^4 atropisomer by the purification procedure. A similar NMR analysis was made for $H_2T_{2\text{-}F}PP$, and we found the amounts to be as follows: α^4, 0.9; $\alpha^3\beta$, 4.0; $\alpha\beta\alpha\beta$, 1.2; $\alpha^2\beta^2$, 2.0. The results indicated a small steric interaction between adjacent 2-fluorophenyl groups.

Column chromatography on basic alumina produced some μ-oxo dimer, but mostly the hydroxide complex, Fe(FPP-3)OH; this was conveniently determined by fluorine NMR and UV/vis spectroscopy. A ^{19}F NMR spectrum in $CDCl_3$ of the porphyrinic material from a chromatography column showed resonances at −78.6, −82.7, and −129.4 ppm (vs. external Freon-F11) indicative of the μ-oxo dimer (FPP-3)FeOFe(FPP-3) and also showed seven other broader resonances (−73.5, −85.1, −98.1, −103.7, −121.4, and −132.4 ppm), indicating the presence of at least two other monomeric α^4 iron porphyrin species. The UV/vis spectrum (λ = 410 and 567 nm) of the solution is similar to those reported for other iron porphyrin hydroxide complexes.[31] By NMR integration, the mixture was less than 30% μ-oxo dimer. Moreover, reacting Fe(FPP-3)X with hydroxide did not produce μ-oxo dimer, unlike the iron picket-fence porphyrins. We were only able to make μ-oxo dimer by reacting Fe^{II}FPP-3 with O_2 under anhydrous conditions. Similarly, Gunter was only able to make a μ-oxo dimer of his iron (nicotinamidophenyl)porphyrin by reacting monomer with trimethylamine *N*-oxide; reactions with hydroxide gave hydroxo complexes.[31] Fe^{II}FPP-3 can be made cleanly under anhydrous conditions by reacting Fe^{III}(FPP-3)X with 1 equiv of $K(BEt_3)H$.

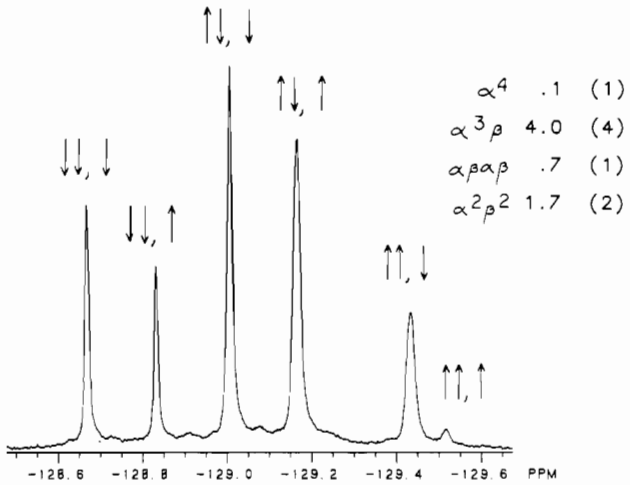

Figure 14. Internal CF_2 resonances for an atropisomeric mixture of H_2FPP-3 in $CDCl_3$. See Table V for the structures represented by the arrows. Relative abundances of atropisomers were measured relative to $\alpha^3\beta$ as 4.0. Statistical ratios are given in parentheses.

It is uncertain how oxygen-atom transfer occurs from iodosobenzene to give the iron–oxo intermediate, but most likely it involves oxygen transfer trans to the halide. Our results with the Fe(TPP)X series suggest that during catalysis the anion either remains coordinated or stays in close proximity to the porphyrin ring. This would explain the lack of shape selectivity we observe with the iron fluoro-pocket porphyrin complexes, since NMR studies indicate that the halide is within the pocket, in agreement with recent crystal structures for iron pocket porphyrin complexes.[32] We observe similar NMR spectra (see Experimental Section) for Fe(FPP-3)Cl and Fe(FPP-3)Br except that the CF_2 resonance adjacent to the carbonyl group is 24 ppm upfield for the bromide complex. With the halide in the pocket, the oxo ligand coordinates to the iron on the open face of the porphyrin, and as a result this catalyst shows no shape selectivity.

Conclusions

While established for manganese,[33] our cyclohexene oxide results provided the first evidence that electron transfer is involved in iron porphyrin catalyzed alkane oxidations.

Subtle changes in catalyst structure give marked changes in selectivities. However, the selectivities for terminal methyl groups thus far with these soluble iron porphyrin catalysts are considerably lower than those observed for the cytochromes P-450 and the ω-hydroxylases with long-chain alkanes.[34] We have observed little or no terminal methyl hydroxylation of *n*-alkanes. It is likely that the enzymatic systems have active-site environments which are considerably more sterically demanding than those possessed by the catalysts used in this study. Suslick et al.,[35] using a (2,4,6-triphenylphenyl)porphyrin manganese catalyst, have observed considerable terminal methyl hydroxylation with *n*-tetradecane. Substituents near the metal center have the advantage of inhibiting the bimolecular self-destruction of the iron porphyrin catalysts, as suggested by Figure 5. It is likely, however, that some catalyst may be lost in an intramolecular process, and if so there should be a slight gain in catalyst lifetimes with increasing bulk of the 2,6-substituents by suppressing a unimolecular pathway.

Our results suggest that a large fraction of the iodosobenzene charged in our reactions is converted into iodoxybenzene. This

(31) Cheng, R.-J.; Latos-Grazynski, L.; Balch, A. L. *Inorg. Chem.* **1982**, *21*, 2412. Gunter, M. J.; McLaughlin, G. M.; Berry, K. J.; Murray, K. S.; Irving, M.; Clark, P. E. *Inorg. Chem.* **1984**, *23*, 283.

(32) (a) Schappacher, M.; Weiss, L.; Montiel-Montoya, R.; Gonser, U.; Bill, E.; Trautwein, A. *Inorg. Chim. Acta* **1983**, *78*, L9. (b) Monteil-Montoya, R.; Bill, E.; Gonser, U.; Lauer, S.; Trautwein, A. X.; Schappacher, M.; Richard, L.; Weiss, R. "The Coordination Chemistry of Metalloenzymes"; Bertini, I., Drago, R. S., Luchinat, C., Eds.; D. Reidel: Dot, The Netherlands, 1983; p 363.

(33) Smegal, J. A.; Hill, C. L. *J. Am. Chem. Soc.* **1983**, *105*, 3515.

(34) McKenna, E. J.; Coon, M. J. *J. Biol. Chem.* **1970**, *345*, 3882.

(35) Suslick, K. S. Pacific Basin ACS Meeting, Honolulu, HI, Dec 19, 1984.

would indicate that efforts to solubilize iodosobenzene by phenyl ring substitution may be counterproduct unless these groups can also be sufficiently bulky to slow down reaction 3 of the proposed mechanism. Bulky groups on the oxidant might reduce the rate of reaction 1, but should increase the overall yield of oxidized hydrocarbon. This behavior with substituted iodosobenzenes has yet to be observed. The fact that iodosobenzene is only sparingly soluble is probably the reason why it is effective at all as an oxygen transfer agent. For the same reason, hydrogen peroxide (H_2O_2) is not a good oxygen transfer agent because iron porphyrins are good catalase mimics and cause its disproportionation.

Both modeling and synthetic efforts in metalloporphyrin-catalyzed hydrocarbon oxidations are continuing.

Experimental Section

Physical Measurements. NMR spectra were recorded on Nicolet 300, Nicolet 360, and Bruker 400 spectrometers. Fluorine resonances are reported vs. external Freon-F11 and in $CDCl_3$ unless otherwise noted. UV/vis spectra were recorded on a Perkin-Elmer 559 instrument interfaced to a Hewlett-Packard HP-87 through an Analytical Computers Smartface interface. All spectra were recorded at 25.0 °C unless specified otherwise. Gas chromatography was done on a Hewlett-Packard instrument 5880 with an FID detector and a Chrompak cross-linked Carbowax capillary column (25 m) and on a Perkin-Elmer Sigma 3 with an FID detector and a Supelco 10% SP-1220 1% phosphoric acid glass-packed column (10 ft).

Materials. DMF (Fisher, reagent grade), heptane (J. T. Baker, HPLC grade), and chloroform (Fisher, Certified) were used as received. Methylene chloride was distilled from P_2O_5; cyclohexane, pentane, octane, methylcyclohexane, *tert*-butylcyclohexane, ethylbenzene, and cyclohexene were distilled from sodium dispersion, and benzene and THF were distilled from sodium dispersion/benzophenone.

Iodosobenzene was made by either chlorine oxidation[36] or peracetic acid oxidation[37] of iodobenzene, followed by base hydrolysis. The product was dried in high vacuum for at least 12 h and stored in a drybox refrigerator (−35 °C). Iodoxybenzene was made by the disproportionation of iodosobenzene.[37] H_2TPP was purchased from Aldrich and purified.[38] Fe(TPP)Cl and Fe(TF_5PP)Cl were purchased from Strem and Aldrich, respectively, and used as received. $H_2T_{4\text{-}Cl}C_1PP$, $H_2T_{4\text{-}Me}PP$, $H_2T_{4\text{-}MeO}PP$, $H_2T_{3\text{-}Me}PP$, $H_2T_{2\text{-}Me}PP$, $H_2T_{2\text{-}F}PP$, and $H_2T_{3,4,5\text{-}MeO}PP$ were made by a published procedure.[39] Fe($T_{4\text{-}Cl}$PP)Cl, Fe($T_{4\text{-}MeO}$PP)Cl, Fe($T_{3,4,5\text{-}MeO}$PP)Cl, Fe($T_{3\text{-}Me}$PP)Cl, and Fe($T_{4\text{-}Me}$PP)Cl were made by the method of Adler and Longo.[39] $FePc(py)_2$,[40] FeFPc,[41] Fe(TPP)MeO,[42] Fe(TPP)Br,[43] Fe(TPP)F,[44] Fe(TPP)ClO_4,[45] Fe($T_{2,4,6\text{-}Me}$P)Cl,[5] Fe($T_{2,4,6\text{-}MeO}$PP)Cl,[46] $H_2T_{AM}PP$,[47] and $FeBr_2$·2THF[48] were made by published procedures.

Oxidation Reactions. The reactions were performed under standard conditions. In a nitrogen-atmosphere drybox, 10 mL of RH/CH_2Cl_2 (3/7) was added to a 25-mL vial containing 0.025 mmol of metalloporphyrin and a magnetic stir bar. While the mixture was being stirred at ambient temperature, iodosobenzene (0.50 mmol) was added all at once and the mixture stirred vigorously for 2 h. It was then removed from the drybox, a 10% solution (2 mL) of sodium bisulfite added to quench further oxidation, and the mixture shaken vigorously. Chlorobenzene (10 μL) was added, the mixture was shaken vigorously and allowed to separate for 15 min, and the organic products were analyzed by GPLC. All yields reported are based on iodosobenzene charged; a yield of 5% corresponds to one catalyst turnover. All reactions were run in at least triplicate and not always with the same batch of iodosobenzene.

Syntheses. ***meso*-α,α,α,α-Tetrakis(heptafluorobutyramidophenyl)porphyrin (FPP-3).** Reagent grade benzene (340 mL) and silica gel 60 (144 g, 230–400 mesh) were added to a 1000-mL round-bottom flask fitted with a nitrogen inlet, reflux condenser, and mechanical stirrer. The apparatus was immersed in an oil bath maintained at 75–80 °C with stirring under nitrogen. After 1 h, $H_2T_{AM}PP$ (5.0 gm) was added and the solution stirred overnight under nitrogen at 76 °C. After cooling to room temperature, the mixture was poured into a flash chromatography column (300 mm × 65 mm) half-filled with silica gel (SG 60). The column was eluted with 3 L of benzene/anhydrous ether dried over sieves (1/1) to remove the $\alpha^3\beta$ isomer, which can be reused, and then 1.5 L of acetone/anhydrous ether (1/1) was added. The first 500 mL of the benzene/anhydrous ether fraction were discarded. The 1-L fractions of acetone/ether were rotovapped to dryness, and 150 mL of methylene chloride dried over sieves was added to the flask. The solution was dried over sodium sulfate, and then heptafluorobutyryl chloride (5 mL) in methylene chloride (20 mL) was added dropwise to the flask. To the kelly green solution was added dropwise a solution of pyridine (5 mL) in methylene chloride (15 mL). The solution was pump–flushed five times quickly and allowed to stir for 18 h. The solution was then poured into 250 mL of water, the organic layer separated, and the aqueous layer extracted with methylene chloride (2 × 200 mL). The combined organic fractions were dried over sodium sulfate and rotovapped to dryness. To the solid were added methylene chloride (50 mL) and heptane (50 mL). Solvent was removed slowly on a rotoevaporator until a precipitate formed, and the flask was refrigerated overnight. Solid was filtered off, washed with pentane, and dried under high vacuum. Yield: 6.50 g, 60.4%. Anal. Calcd for $C_{60}H_{30}N_8O_4F_{28}$: C, 49.40; H, 2.07; N, 7.68; F, 36.46. Found: C, 49.44; H, 2.33; N, 7.62; F, 36.15. MS (fast atom bombardment): *m/e* 1459. ^{19}F NMR (ppm vs. external Freon-F11): −82.3 (3 F, b s), −122.8 (2 F, b s), −128.9 (2 F, b s). UV/vis (nm): 416, 510, 542, 586, 656.

***meso*-α,α,α,α-Tetrakis(perfluorooctanamidophenyl)porphyrin (FPP-7).** The procedure was similar to that described for *meso*-α,α,α,α-tetrakis(heptafluorobutyramidophenyl)porphyrin except for the following. Nine milliliters of perfluorooctanoyl chloride and 9 mL of pyridine were used. Also, methylene chloride (100 mL) was added to this reaction solution, which was poured into 250 mL of water. This was shaken vigorously and then filtered through a medium-filter glass frit. The porphyrin was washed with pentane and methanol. A second crop was obtained by filtering the filtrate, from which more solid had precipitated from the washings of the first crop. Yield: 37.9%. Anal. Calcd for $C_{76}H_{30}N_8O_4F_{60}$: C, 40.41; H, 1.34; N, 4.96; F, 50.46. Found: C, 40.01; H, 1.51; N, 4.89; F, 50.60. UV/vis (nm): 417, 513, 543, 588, 651.

***meso*-α,α,α,α-Tetrakis(*n*-octanamidophenyl)porphyrin (HPP-7).** The procedure was similar to that described for *meso*-α,α,α,α-tetrakis(heptafluorobutyramidophenyl)porphyrin except for the following. Six milliliters of octanoylchloride and 6 mL of pyridine were used. Yield: 50.6%. Anal. Calcd for $C_{76}H_{90}N_8O_4$: C, 77.39; H, 7.69; N, 9.50. Found: C, 77.03; H, 7.68; N, 9.61. UV/vis (nm): 420, 514, 547, 589, 651.

Fe(FPP-3)Br. In a drybox, H_2FPP-3 (2.0 g, 1.37 mmol), $FeBr_2$·2THF (2.5 g, 6.95 mmol), 100 mL of benzene, 100 mL of THF, and 2 mL of 2,6-lutidine were added to a 500-mL round-bottom flask equipped with a reflux adapter and nitrogen inlet. The apparatus was removed from the drybox and attached to a Schlenk line. The solution was heated for 3 h in an oil bath at 80 °C, cooled to room temperature, and exposed to air, and 100 mL of $CHCl_3$ was added. This was then poured into a sepatory funnel containing 200 mL of water. The organic layer was separated and washed with water (2 × 100 mL). The aqueous layer was washed with $CHCl_3$ (2 × 50 mL) and added to the organic extracts, which were dried with sodium sulfate and rotovapped to dryness.

This crude material was purified by flash chromatography on silica gel (SG 60, 300 mm × 60 mm). The column was eluted first with $CHCl_3$ (1000 mL) to remove unreacted porphyrin, which was discarded. This was followed by $CHCl_3$/MeOH (9/1, 1000 mL). A dark brown fraction was collected and rotovapped to dryness. The porphyrinic material was dissolved in 250 mL of chloroform and 65 drops of concentrated HBr added. This was stirred for 2 h, washed with water (2 × 50 mL) and dried with sodium sulfate. The solution was rotovapped to dryness and dissolved in CH_2Cl_2/heptane (1/1, 100 mL). The volume was reduced on a rotoevaporator until a precipitate formed and the flask refrigerated overnight. The solution was filtered and the purple crystals dried in vacuo. Yield: 0.83 g, 38.0%. Anal. Calcd for $FeC_{60}H_{28}N_8O_4F_{28}Br$: C, 45.25; H, 1.77; N, 7.04. Found: C, 45.41; H, 1.75; N, 7.20. ^{19}F NMR ppm vs ext. F11: −47.8 (2F), −55.0 (3F), −111.3 (2F). UV/VIS: 418, 504, 574, 645.

Fe(α^4FPP-3)Cl. The procedure described for Fe(α^4FPP-3)Br was followed except the porphyrinic material isolated from column chroma-

(36) Lucas, H. J.; Kennedy, E. R. "Organic Synthesis"; Wiley: New York, 1955; Collect. Vol. III, p 482.
(37) Sharefkin, J. G.; Saltzman, H. *Org. Synth.* **1963**, *43*, 62.
(38) Barnett, G. H.; Hudson, M. F.; Smith, K. M. *Tetrahedron Lett.* **1973**, 2887.
(39) Adler, A. D.; Longo, F. R.; Kampas, F.; Kim, J. *J. Inorg. Nucl. Chem.* **1970**, *32*, 2443.
(40) Dolphin, D.; Sams, J. R.; Tsin, T. B. *Inorg. Synth.* **1980**, *20*, 155.
(41) Jones, J. G.; Twigg, M. V. *Inorg. Chem.* **1969**, *8*, 2018.
(42) Kobayashi, H.; Higuchi, T.; Kaizu, Y.; Osada, H.; Aoki, M.; *Bull. Chem. Soc. Jpn. 48*, **1975**, 3137.
(43) Baldwin, J. E.; Haraldsson, G. G.; Jones, J. G. *Inorg. Chim. Acta* **1981**, *51*, 29.
(44) Anzai, K.; Hatano, K.; Lee, Y. J.; Scheidt, W. R. *Inorg. Chem.* **1981**, *20*, 2337.
(45) Kobayashi, H.; Higuchi, T.; Eguchi, K. *Bull. Chem. Soc. Jpn.* **1976**, *49*, 457.
(46) Vaska, L.; Amundsen, A. R.; Brady, R.; Flynn, B. R.; Nakai, H. *Finn. Chem. Lett.* **1974**, *66*.
(47) Sorrell, T. N. *Inorg. Synth.* **1980**, *20*, 161.
(48) Ittel, S. D.; English, A. D.; Tolman, C. A.; Jesson, J. P. *Inorg. Chim. Acta* **1979**, *33*, 101.

tography (UV/vis (nm): 410, 567) was dissolved in $CHCl_3$ and treated with 30 drops of water and 30 drops of concentrated HCl. Anal. Calcd for $FeC_{60}H_{28}O_4F_{28}N_8Cl$: C, 46.55; H, 1.82; N, 7.24; F, 34.36; Cl, 2.29. Found: C, 46.42; H, 2.03; N, 7.40; F, 34.35; Cl, 2.51. ^{19}F NMR (ppm vs. external Freon-F11): −64.3 (3 F), −73.0 (2 F), −116.2 (2 F). UV/vis (nm): 415, 498, 570.

Fe(α^4FPP-3) and (α^4FPP-3)FeOFe(α^4FPP-3). In a drybox, $K(Et_3)H$ (320 μL, 1.0 M solution from Aldrich) was added dropwise to a solution of Fe(FPP-3)Cl (0.50 g, 0.32 mmol) in THF (200 mL) at −35 °C. It was warmed to room temperature and stirred for 45 min. The solution was rotovapped to dryness. Dry degassed toluene was added, the solution filtered through a Teflon membrane and the solvent removed in vacuo. The remaining solid was pumped on to remove Et_3B, dissolved in CH_2Cl_2, and crystallized with heptane. Yield: 0.27 g, 55%. ^{19}F NMR (in toluene-d_8, ppm vs. external Freon-F11): −88.6 (3 F, −129.8 (2 F), −134.7 (2 F). UV/vis (nm): 430, 533, 560. The ^{19}F NMR spectrum was also recorded for the bis(pyridine) adduct Fe(FPP-3)$(py)_2$. ^{19}F NMR (in toluene-d_8, ppm vs. external Freon-F11): −81.5 (t, 3 F), −121.3 (q, 2 F), −127.9 (s, 2 F).

To convert the product to the μ-oxo dimer, dry dioxygen was bubbled through a solution of Fe(FPP-3) in dry toluene for 15 min, and then the toluene was removed in vacuo. ^{19}F NMR (ppm vs external Freon-F11): −82.7 (3 F), −123.3 (2 F), −129.4 (2 F). UV/vis (nm): 404, 565.

Fe(α^4FPP-7)Br. The procedure described for Fe(FPP-3)Br was followed. Yield: 0.147 g, 13.9%. Anal. Calcd for $FeC_{76}H_{28}N_8O_4F_{60}Br$: C, 38.15; H, 1.18; N, 4.68; F, 47.64. Found: C, 40.36; H, 1.67; N, 4.65; F, 47.85. UV/vis (nm): 417, 504, 570, 639.

Fe(α^4HPP-7)Br. The procedure described for Fe(FPP-3)Br was followed. Yield: 0.340 g, 30.5%. Anal. Calcd for $FeC_{76}H_{88}N_8O_4Br$: C, 69.50; H, 6.75; N, 8.53. Found: C, 69.61; H, 6.94; N, 8.47. UV/vis (nm): 415, 509, 581.

Fe($T_{2\text{-}Me}$PP)Cl. Iron powder (0.50 gm) and glacial acetic acid (500 mL) were added to a round-bottom flask equipped with a reflux condenser and nitrogen inlet. The apparatus was attached to a Schlenk line and pump–flushed seven times, and the solution was refluxed for 24 h. $H_2T_{2\text{-}Me}PP$ (1.0 g, 1.49 mmol) and NaCl (0.50 g) were added to $CHCl_3$ (25 mL). This mixture was stirred for 15 min and added to the reaction, and the reaction solution was refluxed for 2 h. The volume was reduced to 50 mL and 50 mL of water added. This mixture was sonicated and filtered, and the solid was dried on a high-vacuum line. The crude material was purified by column chromatography on acid alumina, eluting with $CHCl_3$. A light pink band was discarded and was followed by a major dark band, which was collected and rotovapped down to ~100 mL. Heptane (100 mL) was added and the solvent volume slowly reduced on a rotoevaporator until a precipitate formed, and then the mixture was refrigerated overnight. Yield: 0.537 g, 44.8%. Anal. Calcd for $FeC_{48}H_{36}N_4Cl$: C, 75.85: H, 4.77; N, 7.37; Cl, 4.66. Found: C, 76.01, H, 5.25; N, 7.10; Cl, 4.88. UV/vis (nm): 376, 415, 507, 575.

Fe($T_{2,4,6\text{-}MeO}$PP)Cl (E26585-17). The procedure described for Fe($T_{2\text{-}Me}$PP)Cl was followed. Yield: 74.4%. UV/vis (nm): 418, 509, 586.

Acknowledgment. We thank V. C. Cannelongo, J. A. Mohring, and J. B. Jensen for expert technical assistance. We are also grateful to our colleagues for many stimulating discussions and to P. J. Domaille and D. C. Roe for help with NMR measurements.

Registry No. Fe($T_{4\text{-}Me}$PP)Cl, 19496-18-5; Fe($T_{3\text{-}Me}$PP)Cl, 52155-49-4; Fe($T_{2\text{-}Me}$PP)Cl, 52155-50-7; Fe($T_{3,4,5\text{-}MeO}$PP)Cl, 81245-21-8; Fe($T_{2,4,6\text{-}MeO}$PP)Cl, 53470-05-6; Fe($T_{2\text{-}F}$PP)Cl, 98858-68-5; Fe($T_{F\text{-}5}$PP)Cl, 36965-71-6; Fe(α-FPP-3)Cl, 98858-69-6; Fe(α-FPP-3)Br, 98858-70-9; Fe(α-FPP-7)Br, 98858-71-0; Fe(α-HPP-7)Br, 98858-72-1; FePc, 132-16-1; FeFPc, 23844-93-1; Fe(TPP)Cl, 16456-81-8; cyclohexane, 110-82-7; *n*-pentane, 109-66-0; *n*-octane, 111-65-9; methylcyclohexane, 108-87-2; *tert*-butylcyclohexane, 3178-22-1; ethylbenzene, 100-41-4.

Contribution from the Department of Chemistry, Memorial University of Newfoundland, St. John's, Newfoundland, Canada A1B 3X7, and The Chemistry Division, National Research Council,† Ottawa, Ontario, Canada K1A 0R6

Binuclear Copper(II) Complexes of a Series of Tetradentate Pyrazolyldiazines. Crystal and Molecular Structures of [μ-3,6-Bis(3,5-dimethyl-1-pyrazolyl)pyridazine-N,μ-N^3,μ-$N^{3'}$,N](μ-hydroxo)dichlorodicopper(II) Aquotrichlorocuprate Hydrate, $Cu_3C_{14}H_{21}Cl_5N_6O_3$, and [μ-3,6-Bis(3,5-dimethyl-1-pyrazolyl)pyridazine-N,μ-N^6,μ-N^7,N](μ-hydroxo)tris(nitrato)diaquodicopper(II) Hydrate, $Cu_2C_{14}H_{23}N_9O_{13}$

Laurence K. Thompson,*[1a] T. C. Woon,[1a] David B. Murphy,[1a] Eric J. Gabe,[1b] Florence L. Lee,[1b] and Y. Le Page[1b]

Received January 23, 1985

Binucleating pyrazolylpyridazine and phthalazine ligands form predominantly binuclear copper(II) complexes in which, in many cases, the metal centers are bridged by a hydroxide group in addition to the diazine bridge. Low magnetic moments for these species (μ_{eff}(room temperature) < 0.74 μ_B) indicate strong spin exchange between the copper(II) centers. One complex, Cu_2(PPD)(OH)Br_3·1.5H_2O (PPD = 3,6-bis(1-pyrazolyl)pyridazine), was found to be diamagnetic at room temperature. The crystal and molecular structures of $[Cu_2(PPDMe)(OH)Cl_2][CuCl_3(H_2O)]\cdot H_2O$ (V) and $[Cu_2(PPDMe)(OH)(NO_3)_2(H_2O)_2](NO_3)\cdot H_2O$ (VII) (PPDMe = 3,6-bis(3,5-dimethyl-1-pyrazolyl)pyridazine) are reported. The trinuclear species (V) contains the unusual tetrahedrally distorted anion $[CuCl_3(H_2O)]^-$ and a binuclear hydroxo-bridged cation. V crystallized in the monoclinic system, space group *Am*, with a = 7.4942 (4) Å, b = 20.418 (1) Å, c = 7.5092 (5) Å, β = 90.93 (1)°, and two formula units per unit cell. VII crystallized in the monoclinic system, space group $P2_1/c$, with a = 6.787 (2) Å, b = 20.986 (3) Å, c = 16.825 (3) Å, β = 95.49 (2)°, and four formula units per unit cell. Refinement by full-matrix least squares gave final R factors of 0.039 for both systems. The copper centers in the binuclear cation in V are close to square planar with a bridging hydroxide angle of 126.0 (5)° and a Cu---Cu separation of 3.384 (2) Å. In VII the copper centers are considered to be distorted four-coordinate with axial contacts greater than 2.3 Å, a bridging hydroxide angle of 119.3 (2)°, and a Cu---Cu separation of 3.338 (1) Å. Variable-temperature magnetic studies on both complexes indicate strong antiferromagnetic exchange in both cations.

Introduction

Tetradentate phthalazine,[2-18] pyridazine,[3-5,19-23] and pyrazole ligands[3] have been shown to generate principally binuclear transition-metal complexes. Many of the copper(II) derivatives of the phthalazine systems have multiple bridges between the metal centers, including a hydroxide bridge, which is considered to be

* To whom correspondence should be addressed.
† NRC No. 25059.

(1) (a) Memorial University. (b) National Research Council.
(2) Andrew, J. E.; Blake, A. B. *J. Chem. Soc. A* **1969**, 1408.
(3) Ball, P. W.; Blake, A. B. *J. Chem. Soc. A* **1969**, 1415.
(4) Andrew, J. E.; Ball, P. W.; Blake, A. B. *J. Chem. Soc., Chem. Commun.* **1969**, 143.
(5) Ball, P. W.; Blake, A. B. *J. Chem. Soc., Dalton Trans.* **1974**, 852.

0020-1669/85/1324-4719$01.50/0